

ISTITUTO NAZIONALE DI FISICA NUCLEARE
Laboratori Nazionali di Frascati

LNF-78/15(R)
20 Marzo 1978

M. Bassetti, M. E. Biagini, R. Boni, A. Cattoni, V. Chimenti,
E. Fiorentino, S. Guiducci, G. Martinelli, M. A. Preger,
C. Sanelli, M. Serio, S. Tazzari and F. Tazzioli: A. L. A. -
1.2 GeV HIGH LUMINOSITY ELECTRON-POSITRON
STORAGE RING. DESIGN STUDY.

M. Bassetti, M. E. Biagini, R. Boni, A. Cattoni, V. Chimenti, E. Fiorentino, S. Guiducci, G. Martinelli, M. A. Preger, C. Sanelli, M. Serio, S. Tazzari and F. Tazzioli: **A.L.A. - A 1.2 GeV high luminosity electron-positron storage ring. Design study.**

1. - Introduction

The construction of a high-luminosity electron-positron storage ring, in the center of mass energy range between 900 and 1700 MeV, has recently been proposed. In the preliminary proposal¹⁾ it was suggested that a luminosity from one to two orders of magnitude higher than that obtainable from machines presently operating in the above energy range, was achievable.

The design study presented in this paper confirms the preliminary proposal¹⁾ conclusions over an energy range that has been extended to 2400 MeV. The proposed machine (A.L.A.) is an e^+e^- storage ring with a maximum energy of 1.2 GeV per beam, two 3 m long interaction straight sections, and a luminosity around $10^{31} \text{ cm}^{-2} \text{ s}^{-1}$ in between .8 and 1.2 GeV per beam.

High luminosity is mainly obtained:

- by making the vertical betatron functions, β_z^* at the interaction point low (low- β);
- by means of an optical structure, that allows the "invariant" M^* ²⁾ to be changed as a function of the operating energy.

The "low β " technique is well understood and experimentally proven. The method of varying M^* , so as to cover a large energy range with a luminosity (in our case) proportional to the beam energy, $L \propto E$, although it has not yet been exploited on existing machines, is related to very simple and well understood principles, and should present no special problems. The method has been included, in various forms, in the most recent projects^{3),4),5)}

In the ALA design, high values of M^* are associated with values of α_c (momentum compaction) higher than those generally used. Our maximum value of α_c , is however not too far from that ($\alpha_c = .17$) of the Russian ring VEPP 2-M⁶⁾. The stability of the structure in all three dimensions, is guaranteed by letting the field index in the bending magnets (n) be equal to .5.

The following limits have been also set:

1. - Maximum current: 150 mA per beam.
2. - Maximum beam-beam linear tune shift: $\xi_M = .06$.

The limit on the maximum storable current (on which the maximum obtainable luminosity depends) is determined both by the injection rate, and by an educated guess on the maximum current per beam that can

be stored without too many longitudinal stability problems.

Normal operation is with one bunch per beam, but the magnetic structure and the RF system do allow for two bunch-operation.

The maximum value of the interaction parameter, ξ , is consistent with the values obtained by operating storage rings^{7), 8), 9), 10)} and with the design values assumed for PEP⁴⁾ and PETRA.⁵⁾

The maximum peak currents (given the maximum current stored in one bunch and the RF frequency) are much lower than those obtained at SPEAR and only a few times larger than those that have been run at ADONE.

The installation on Adone of a 51.4 MHz RF system identical to that proposed for ALA, will allow the assumption on the maximum storable current to be tested.

A problem encountered in operating Adone is the very strong dependence of luminosity on energy ($L \propto E^7$) below ~ 900 MeV (the expected natural behaviour is $L \propto E^4$). Although the departure from linear beam-beam theory has not been understood in detail, it has been suggested⁵⁾ that it could be explained by a diffusion process, in competition with radiation damping. Since the damping time at a given energy is inversely proportional to the bending magnet radius (ρ), ALA is designed to have a short bending radius, ($\rho = 2.5$ m) by letting the field in the bending magnets be equal to 1.6 T. The damping time at a given energy is about three times shorter than that of Adone. It is therefore expected that ξ_M will stay constant as a function of energy above ~ 500 MeV.

As far as injection is concerned, we remark that at the present design study level, it is still an open question whether it will be more convenient, from the point of view of cost, performance and interference with other activities, to inject into ALA directly from our linear accelerator, or to use ADONE as a booster. Here too more information will be provided by the experience with the 51 MHz RF cavity to be installed in Adone.

The machine lay-out is shown in figure 1),

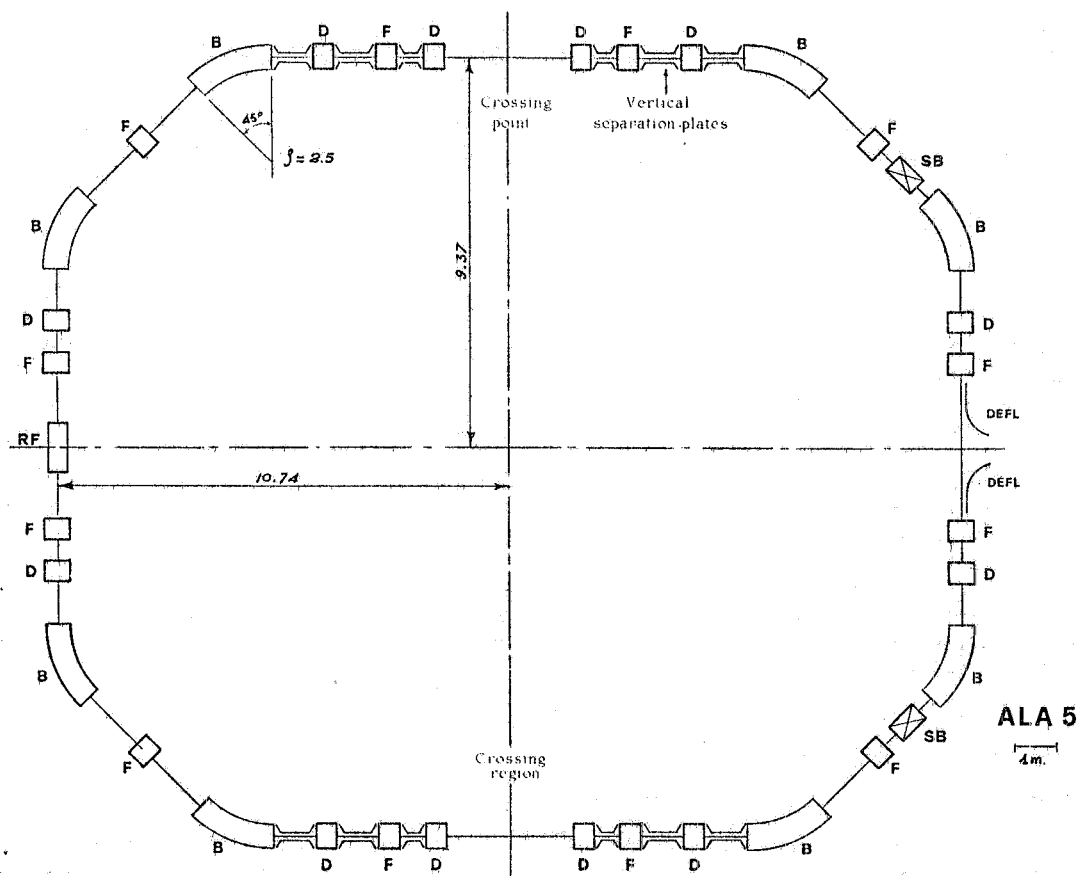


Fig. 1 - Ring layout.-

2. - DESIGN CRITERIA

2.1. - For a relatively low energy ring like ALA the stored electrons radiation energy loss is also relatively low, so that the choice of a bending radius for a given maximum energy is not critical. A small radius has the advantage of shortening the overall length of the ring and increasing the damping of synchrotron and betatron oscillations.

Because all instabilities compete with damping and since damping is also expected to affect the dependence of luminosity on energy (as it has been explained in the introduction), we propose for ALA a bending radius of 2.5 m, which is the minimum value that can be had for a maximum energy of 1.2 GeV and a bending field not exceeding 1.6 Tesla.

2.2. - Let us recall that the maximum luminosity can be expressed as follows:

$$L = K_L \frac{E^4}{RQ} M^* h \xi_M^2 \left(\frac{1}{\beta_x^*} + \frac{1}{\beta_z^*} \right) \text{cm}^{-2} \text{s}^{-1} \quad (1)$$

where:

$K_L = 1.06 \times 10^{38} \text{s}^{-1} \text{GeV}^{-4}$ and depends only on the chosen units
 R, Q are the average radius and the bending radius respectively (cm)
 M^* is an optical parameter which determines the beam cross section at the interaction point (cm)
 h is the number of bunches per beam
 β_x^*, β_z^* are the betatron functions at the interaction point (cm)
 ξ_M is the maximum linear tune shift.

If we assume ξ_M to be independent of E , it follows that, for a given optical structure and for a given number of bunches, luminosity is proportional to the fourth power of energy ($L \propto E^4$).

The number of particles to be stored in order to obtain the luminosity given by (1) is

$$N = K_N \frac{E^3}{Q} M^* h \xi_M \quad (2)$$

where $K_N = 6.41 \times 10^{12} \text{GeV}^{-3}$ and depends only on the chosen units.

Dividing (1) by (2) the "specific luminosity" is obtained:

$$\frac{L}{N} = \frac{K_L}{K_N} \frac{\xi_M}{R} E \left(\frac{1}{\beta_z^*} + \frac{1}{\beta_x^*} \right) \quad (3)$$

The number of particles (and hence the stored current) must also stay below the so-called longitudinal limit¹⁾ which, in our case, is always higher than the transverse limit given by (2).

2.3. - The design aims are:

a) High luminosity at maximum energy.

Injection and longitudinal instabilities set a limit on the number of particles that can be stored; the maximum luminosity is therefore proportional to the specific luminosity. We assume $I_{\max} = 150 \text{mA}$.

From (3) it can be seen that the specific luminosity increases when R and $\beta_{x,z}^*$ are decreased ("low β "). A low R is always convenient. A lower limit on R is however set by the length of the bending magnets, free space for experiments, injection, RF cavities, controls and other beam optics requirements. In the ALA design R is 11.14 m.

For optics reasons it is convenient to make β_z^* very low and β_x^* lower than its average value in the machine, but higher than β_z^* . It is however useless to make β_z^* lower than the bunch length. For ALA we set $\beta_z^* = .2 \text{ m}$, $\beta_x^* = 1 \text{ m}$,

The value of ξ_M (which appears in (3)) is a natural limit, deduced from experimental observations on existing machines. We assume $\xi_M = .06$, in agreement with existing experimental data.^{7), 8), 9), 10)}

The specific luminosity and the number of stored particles being thus determined, the value of $(M^* h/\rho)$ at maximum energy is obtained from (2). The choice of $\rho = 2.5 \text{ m}$ has been already discussed. Operation with more than 1 bunch per beam complicates the longitudinal stability problem, and requires the beams to be kept separate in all crossing points along the machine where β_z is higher than β_z^* . In the present design we therefore assume $h = 1$ leaving the possibility of letting h become 2, if it will be concluded, on the basis of further work, that it is convenient.

ρ and h being fixed, the value of M^* at the maximum energy is determined. We assume to store a maximum number of particles $N_{\text{max}} = 2.2 \times 10^{11}$ (corresponding to 150 mA per beam), and get $L(E_{\text{max}}) = 1.4 \times 10^{31} \text{ cm}^{-2} \text{ s}^{-1}$; from (1) one then obtains $M^*(E_{\text{max}}) = .82 \text{ m}$.

b) Luminosity versus energy slope.

For energies lower than E_{max} it is necessary to increase of $M^*(E_{\text{max}})$ if the slope of $L(E)$ is to be decreased with respect to the natural E^4 dependence (see (1)). Assuming the optical structure is capable of providing any desired value of M^* , one could let M^* depend on E as follows:

$$M^* = M_{E_{\text{max}}}^* (E/E_{\text{max}})^{-n} \quad (4)$$

From (1) and (2) one then gets:

$$L = L_{E_{\text{max}}} (E/E_{\text{max}})^{4-n} \quad N = N_{E_{\text{max}}} (E/E_{\text{max}})^{3-n} \quad (5)$$

and the beam transverse dimensions are given by

$$\sigma = \sigma_{(E_{\text{max}})} (E/E_{\text{max}})^{\frac{2-n}{2}} \quad (6)$$

If the number of stored particles is constant, and equal to $N_{E_{\text{max}}}$, n must be equal to 3. With this choice we get

$$\begin{cases} N = \text{const} = N_{\text{max}} \\ M^* = M_{E_{\text{max}}}^* (E_{\text{max}}/E)^3 \end{cases} \quad \begin{cases} L = L_{E_{\text{max}}} (E/E_{\text{max}}) \\ \sigma = \sigma_{E_{\text{max}}} (E_{\text{max}}/E)^{1/2} \end{cases} \quad (7)$$

Formulae (7) hold as long as the optical structure and the acceptance allow M^* to follow law (4).

The structure of ALA allows M^* to be varied continuously between .3 and 4 meters, at fixed Q_x and Q_z . Moreover, all operating structures can be reached from the injection configuration.¹²⁾ Other considerations (see Section 3) constrain M^* to stay below $\sim 3 \text{ m}$. A luminosity decreasing linearly with energy is thus obtained in between 1200 MeV and about 800 MeV. Below 800 MeV the behaviour of L is the natural one (proportional to the fourth power of energy) as shown in fig. 2).

2.4. - A beam parameter very important for high energy physics experiments is bunch length. The proposed optical structure and RF frequency lead to the "natural" (r.m.s.) source length as a function of energy shown in fig. 3).

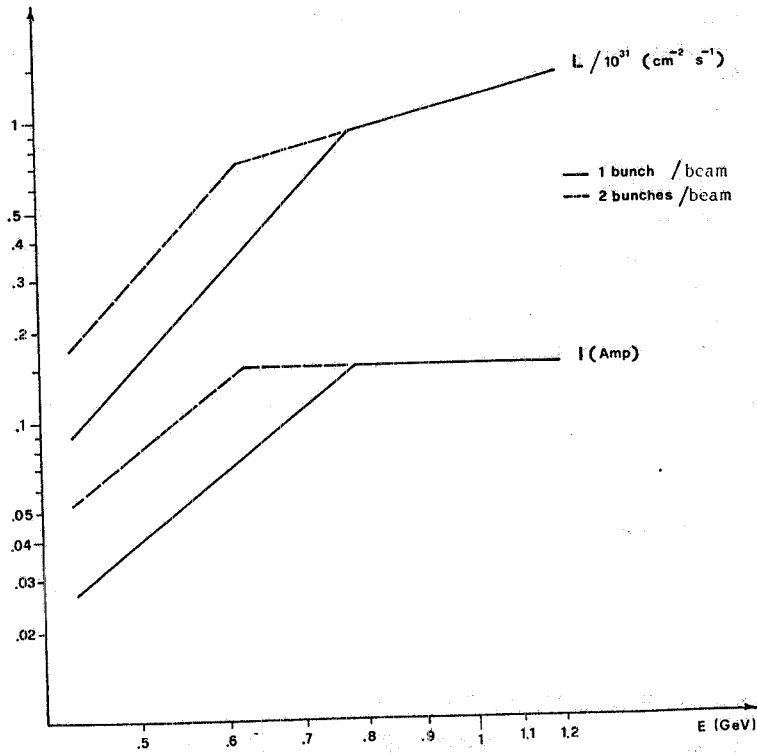


Fig. 2 - Luminosity and total current as a function of energy.-

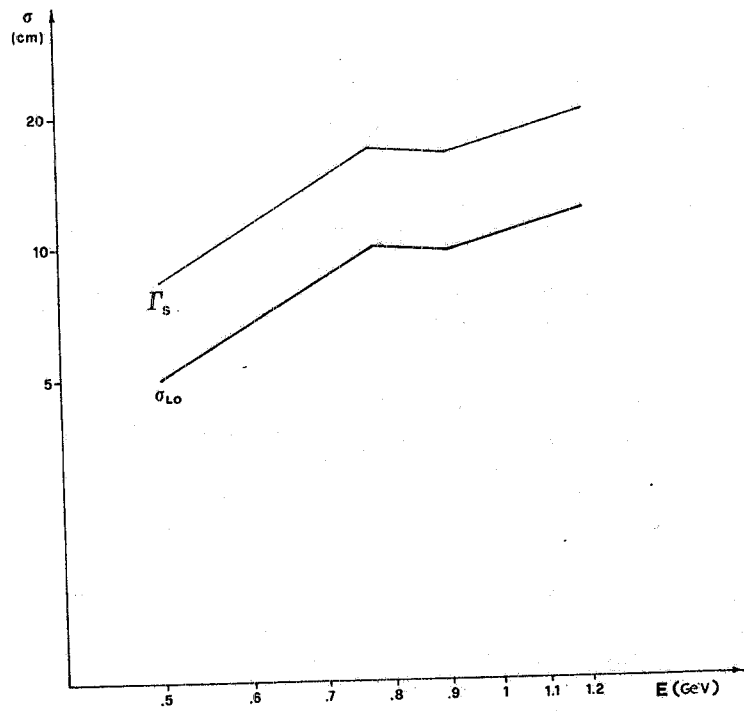


Fig. 3 - Natural r.m.s. bunch length (250 KV) σ_{Lo} and source distribution Γ_s (FWHM).-

All existing storage rings however exhibit an anomalous bunch lengthening^{13),14),15)} A complete theory of the effect is not available, but according to recently developed models¹⁶⁾ one can try to extrapolate from the existing data.

Scaling from ADONE¹⁷⁾ the obtained lengthening is negligible. Allowing for the uncertainties of the procedure and the limitations of the model, an upper limit of a factor of 1.5 ± 2 over the natural dimensions at ~ 800 MeV can be set. The natural bunch and source lengths versus energy are shown in Fig. 3). A very careful vacuum chamber design should make it possible to further improve this figure.

A source length much shorter than that indicated in Fig. 3) would call for a higher RF frequency, implying higher costs and a certain amount of development work. A brief discussion of the possibility of raising the RF frequency (which also allows β_z^* minimum to be lowered and therefore the maximum luminosity to be increased) is given in Appendix 1.

Another important parameter is the c.m. energy resolution. With the proposed bending radius, the FWHM of the center of mass energy distribution is

$$\Gamma_E^{(cm)} = .45 E_{GeV}^{(cm)} \text{ MeV} \quad (8)$$

3. - OPTICAL STRUCTURE

3.1. - Summarizing the conclusions of the preceding Section, the optical structure must:

- a) allow for low values of β_x, β_z at two crossing points ($\beta_x^* = 1 \text{ m}, \beta_z^* = .2 \text{ m}$)
- b) allow M^* to be varied over a factor of at least 4
- c) have $\varrho = 2.5 \text{ m}$
- d) keep R as low as possible.

It is also necessary to make the betatron wave numbers, Q_x and Q_z , not too low and preferably odd. The design figures are $Q_x = Q_z = 3.2$ and are practically the highest obtainable with the proposed structure.

Since at injection β_z^* has to be higher than in operation, an injection configuration from which the operating configuration can be smoothly reached is also required.

The described project aims must be obtained taking into account some important constraints such as:

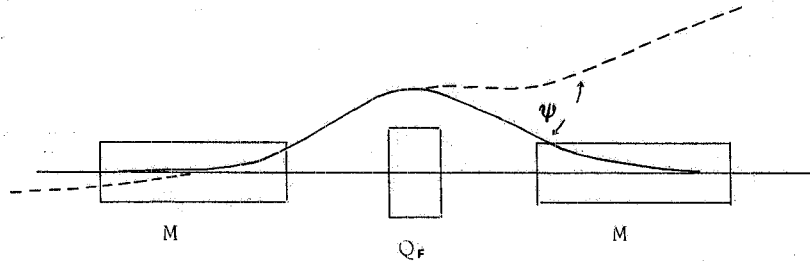
- e) free length of interaction straight sections $\geq 3 \text{ m}$
- f) straight sections conveniently located along the ring for injection, RF cavities, beam separation at injection, and control instrumentation
- g) cost minimization and non critical operation (in practice the maximum values of β_x, β_z and ψ should be not too high and conveniently located along the machine).

3.2. - In low- β storage rings the optical structure is usually divided in two parts: low- β insertion and periodic structure; in order to leave the optical functions in the periodic part unperturbed, it is necessary to match them to those of the low- β insertion. This requirements is fulfilled by letting the insertion have as many degrees of freedom (normally number of quadrupoles) as the number of conditions to be satisfied. It must be kept in mind, however, that a large number of degrees of freedom, and hence of quadrupoles, increases the length and cost of the storage ring.

For long machines, such as SPEAR, PEP or PETRA, the insertions are a relatively small fraction of the whole machine; this is not true for short machines such as ALA. For ALA it is therefore not convenient to design a matched structure; each machine quadrant should be looked at as an insertion with bending magnets, matched to the next quadrant by symmetry only. In this way the conditions to be met in a machine quadrant are only 4, namely $\beta_x^*, \beta_z^*, Q_x$ and Q_z , and no constraint is set on the values of β at the

symmetry point. However, if only 4 quadrupoles per quadrant are provided, there is no possibility of varying M^* .

In order to fulfill condition b) a quadrupole symmetrically placed between the two magnets of each quadrant and controlling the value of the dispersion ψ (see figure) is added.



It is also convenient to add a sixth quadrupole, mainly to satisfy condition g) at constant β_x , β_z , Q_x , Q_z , M^* .

3.3. - The resulting optical structure is shown in Fig. 1. The values of M^* are given, as a function of energy, in fig. 4a. Fig. 5 shows functions β_x , β_z and ψ for the extreme cases $M^* = 3 \text{ m}$ and $M^* = .82 \text{ m}$.

Fig. 4b shows the behaviour of the momentum compaction, α_c as a function of energy (namely for the different configurations corresponding to the different working energies). The bunch length, and therefore the source length, depend on α_c . The damping partition numbers are independent of α_c if the field index of the bending magnets is $n = .5$.

Since the source length is a very important parameter, it is not convenient to increase α_c (and hence M^*) too much. We have set $\alpha_{c_{\max}} = .25$.

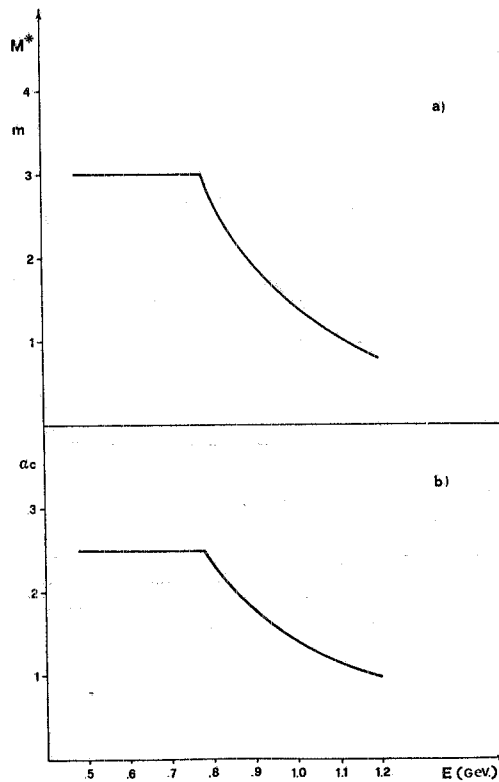


Fig. 4 - M^* , α_c as a function of energy. -

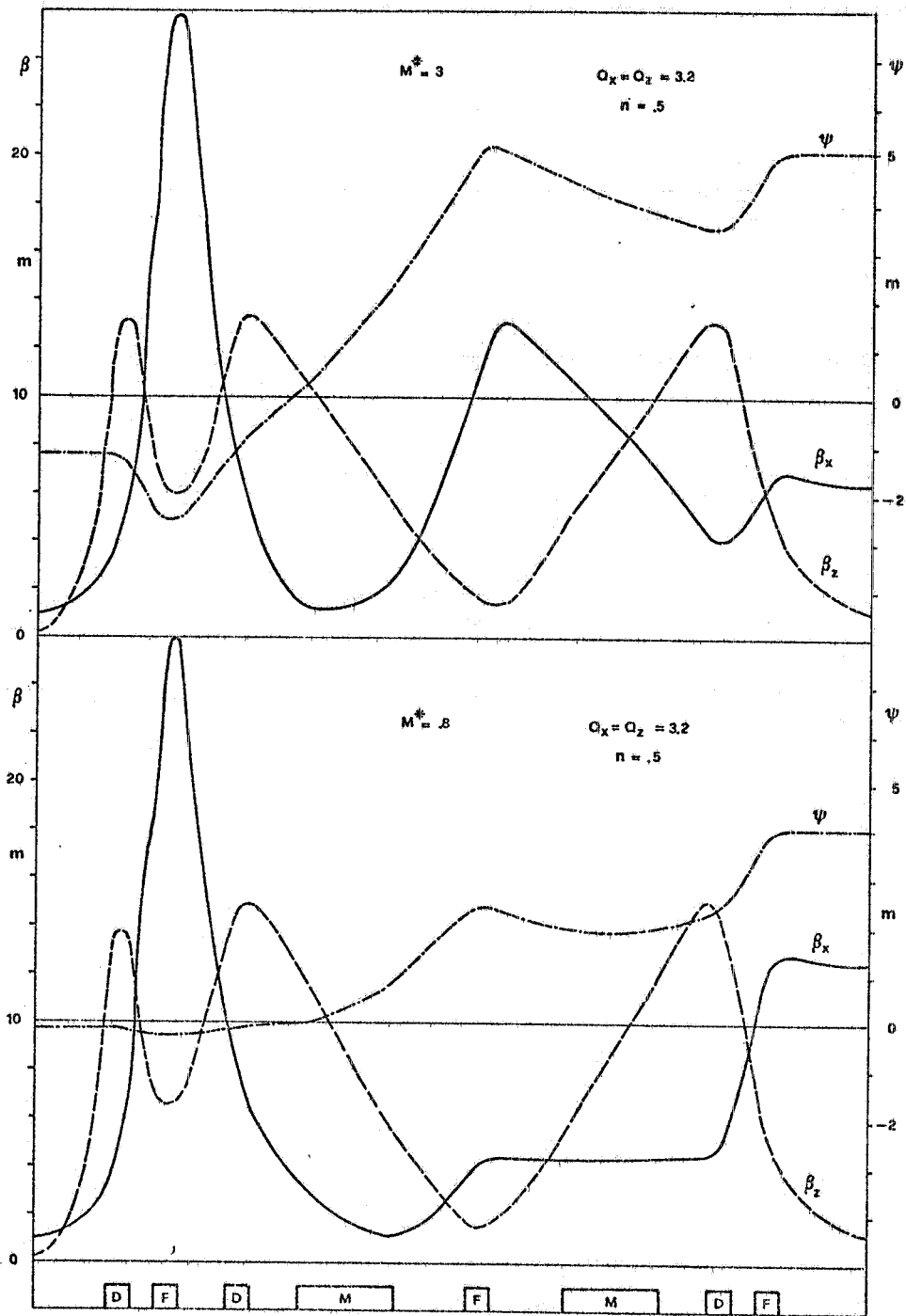


Fig. 5 - Optical functions.-

3.4. - Aperture.

3.4.1. - The aperture requirements are set by beam dimensions in the operating configurations and by injection.

The maximum required aperture for operation occurs at about 800 MeV, where beam dimensions are largest.¹⁸⁾ In order to calculate it, we have assumed to leave a free aperture for the beam (in interaction) of at least $\pm 8\sigma$, σ being the natural r.m.s. transverse dimension of the beam itself. In addition ± 5 mm must be added in order to allow for residual closed orbits and ± 15 mm for the vacuum chamber (with bake-out) and assembly tolerances. In the vertical direction, one also has to consider beam separation at the crossing point.

It is assumed, according to present knowledge,¹⁹⁾ that bunch lengthening does not appreciably affect the required aperture.

From the above considerations we get the following indicative values for the aperture:

	Horizontal	Vertical
Quadrupoles	150 mm	80 mm
Magnets.....	150 mm	70 mm

Particularly important, from the point of view of costs, is to keep the magnet gap as low as possible.

3.4.2. - The apertures required for injection are much lower than those computed in 3.4.1 if ADONE is used as a booster for injecting positrons.

If instead positrons are to be injected directly from the LINAC the indicated apertures are critical all around²⁰⁾ and, in any case, at least 8 quadrupoles in the "injection bump" region must be enlarged to ~ 200 mm diameter.

A more detailed study of all aspects of the problem is needed before deciding whether to use ADONE or enlarge the machine aperture.

3.5. - The proposed optical structure is rather flexible. In particular, it is possible to cover the entire Q_x , Q_z range in between 2 and 3.3.

The main structure parameters are listed in Table 1.

- Table 1 -

OPTICS PARAMETERS		
N. of periods	2	
N. of crossings	2 x 3 m	
N. of magnets	8	
N. of quadrupoles	24	
Circumference	70 m	
Bending radius (ρ)	2.5 m	
Horizontal betatron wave number	3.2	
Vertical betatron wave number	3.2	
	Interaction configuration	Injection configuration
Invariant (M)80 \pm 2.28 m	.55 m
Invariant at crossing (M^*)81 \pm 3.00 m	.80 m
Momentum compaction (α_c)10 \pm .25	.036
Horizontal betatron wavelength at crossing (β_x^*)	1 m	3 m
Vertical betatron wavelength at crossing (β_z^*)2 m	1 m
Dispersion at crossing (ψ^*)	-.16 \pm -1.21 m	1.2 m
β_x^{max}	26.9 \pm 27.4 m	17.9 m
β_z^{max}	13.3 \pm 15.3 m	24.5 m
ψ^{max}	4.0 \pm 5.1 m	4.3 m
Horizontal chromaticity ($p\Delta v_x/v_x\Delta p$)	-2.30 \pm -2.67	-1.38
Vertical chromaticity ($p\Delta v_z/v_z\Delta p$)	-1.53 \pm -1.91	-1.77

Note: A * indicates value at x-ing point.-

3.6. - Hexapoles.

The introduction of hexapolar corrections is desirable to cure the head-tail instability.²¹⁾ It is sufficient to provide two families of hexapoles, which can invert the natural chromaticity of the ring, bringing it to small positive values.

The chromaticities of ALA, as shown in Table 1), are not high and their correction with two families of 4 hexapoles is not too difficult.²²⁾

Since hexapoles introduce non-linearities which can reduce the effective aperture, their final location on the ring will be determined by means of tracking programs.^{23),24)}

4. - MAGNET SYSTEM

4.1. - General description.

Bending magnet and quadrupole cores are designed to be of laminated construction (glued laminations). The selection of a laminated structure is justified in Ref. 5),

The bending magnet core is C-shaped since this gives definite advantages, such as ease of assembling and accessibility to the vacuum chamber, over an H-shaped core.

Symmetry requirements and equipment cost reduction require the quadrupole cores to be constructed in 4 parts (the standard lamination comprising one pole and 1/4 of the yoke). Modern techniques allow the 4 parts to be assembled very economically by means of welded-on connecting plates. The need for fast access to the vacuum chamber makes it preferable to assemble the core in two separable halves, symmetrical with respect to the horizontal plane. Assembly tolerances and position reproducibility will be guaranteed by reference pins on the plates coupling the two halves.

4.2. - Power supply.

The optimized current density results from the minimization of several costs such as:

- power consumption and cooling
- coil dimensions and construction
- core size and construction.

The optimization has been performed on the basis of 50.000 running hours, and, at present costs, a current density of about 5 A/mm² is selected. The resulting power needs are:

- bending magnets P = 500 KW I = 1600 A
- quadrupoles P = 230 KW to be divided among different power supplies with maximum currents lower than 600 A.

The technical solution selected for the power supplies is a 12 phase SCR rectifier bridge, keeping the current ripple below 1/10⁴. Regulation is provided by high gain feedback loops on the SCR's. The output current is regulated to better than 1/10⁴.²⁵⁾

4.3. - Alignment.

Since we are considering a storage ring similar to ADONE, with an accessible center, it seems reasonable to rely on the same methods used at that time, such as precision theodolite, precision level and invar wires for direct distance measurements. Obviously, the problem can be solved even if the machine center is not accessible, by constructing a reference figure made out of polygons conveniently connected each other and repeated along the ring.

A detailed alignment plan has not been designed at this stage of the project; general criteria are discussed in Ref. 26) and 27).

Bending magnet and quadrupole characteristics are listed in Table 2.

- Table 2 -

MAIN CHARACTERISTICS	BENDING MAGNET ²⁸⁾	QUADRUPOLE LENS ²⁹⁾
Gap height	70 mm	-
Gap width	300 mm	-
Free diameter	-	150 mm
Core magnetic length	1963 mm	500 mm
Bending radius	2500 mm	-
Maximum field or gradient	16 K Gauss	800 Gauss/cm
Nominal current	1562 A	412 A
Resistance (60°C)	0,0246 Ohm	0,0552 Ohm
Unit power	60 KW	9,5 KW
Turns per pole	32	50
Conductor cross section	18 x 18 mm ²	12 x 12 mm ²
Cooling hole \varnothing	9 mm	7 mm
Water circuits	4	4
Δt cooling water	20°C	20°C
Pressure drop	11 Ate	< 11 Ate
Water flow	45 l/min	7 l/min
Core weight	12 tons	0,63 tons
Coil weight	0,75 tons	0,28 tons

Cross sections of bending magnet and quadrupole cores are shown in figs. 6) and 7).

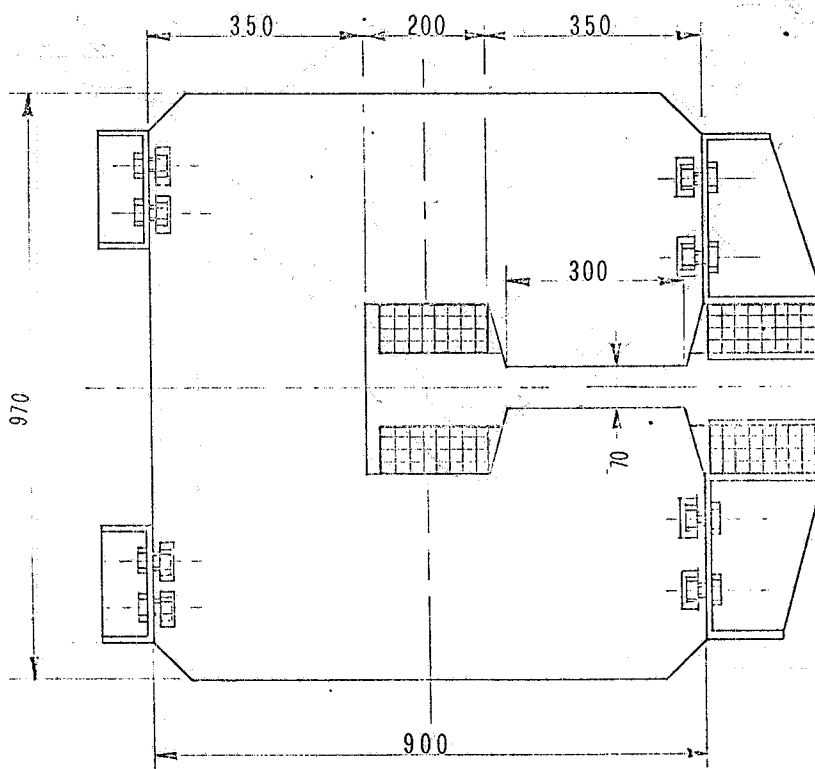


Fig. 6 - Bending magnet.--

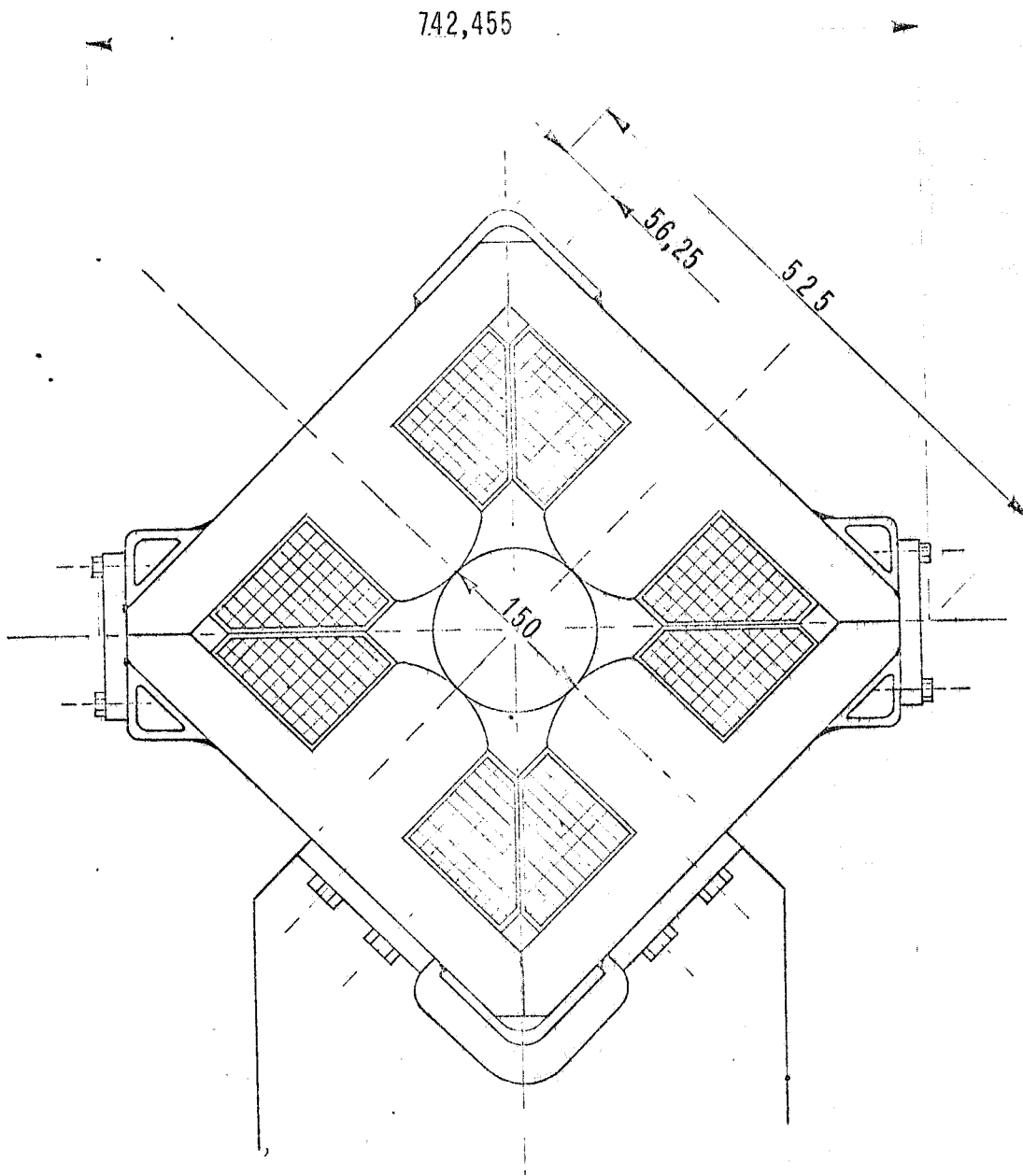


Fig. 7 - Quadrupole.-

5. - VACUUM SYSTEM

5.1. - General description.

The total outgassing rate due to synchrotron radiation is given by:

$$Q = 1.93 \times 10^{-3} i D \gamma \left[1 - \left(\frac{\epsilon_0}{\epsilon_c} \right)^{1/3} \right]$$

Q = total outgassing rate in Pa.l/sec (1 Pa = 7.5×10^{-3} torr)

i = total stored current in mA

D = desorption efficiency in molecules/photon

γ = beam energy/electron rest mass

ϵ_0 = photon energy threshold for desorption (~ 10 eV)

ϵ_c = critical energy of synchrotron radiation spectrum: $\epsilon_c = \frac{3}{2} \frac{\hbar c \gamma^3}{\rho}$

Introducing ϵ_c in the above expression of Q one gets:

$$Q = 1.93 \times 10^{-3} i D (\gamma - 316 \sqrt[3]{\rho}) \quad (\rho \text{ in meters})$$

Taking for D the value measured at Adone, $D = 3 \times 10^{-6}$ mol/photon (this value can be decreased by means of particular treatments such as Argon glow-discharge) we get at maximum current and maximum energy:

$$Q = 3.33 \times 10^{-3} \text{ Pa} \cdot \text{l/sec}$$

Taking into account the apertures of the magnetic elements indicated in Table 2 and the dimensions of other machine parts such as bump, inflector, RF cavity, beam instrumentation, fittings, pumps, etc.), the vacuum chamber overall inside area is:

$$A_t \simeq 10^6 \text{ cm}^2$$

Assuming the specific outgassing rate (without beam) after bake-out is $q = 10^{-10}$ Pa.l/s.cm one gets a total outgassing $Q = qA_t = 10^4$ Pa.l/sec.

For a final limit pressure of 2×10^{-8} Pa without beam the required overall pumping speed is:

$$S = Q/p = 5 \times 10^3 \text{ l/s}$$

In addition, the outgassing rate due to synchrotron radiation is about 30 times larger than the no-beam vacuum chamber rate and occurs mainly inside and near bending magnets; distributed pumping in the bending field is therefore required to take care of the beam induced load. Titanium sublimators at suitable points along the machine may be also added.

A better vacuum in the experimental straight section can be easily obtained because of the favourable machine geometry: the gas source is in the bending magnets, relatively far from the crossing point, and the impedance between magnets and interaction straight section is high. A suitable pump distribution will ensure a ten-fold pressure drop.

All calculations are made for a stainless steel vacuum chamber. In the final design, however, an alternative solution with an aluminium vacuum chamber should be carefully studied.

5.2. - Fore-vacuum system.

We assume an average initial specific outgassing $q = 10^{-6}$ Pa.l/s.cm, so that:

$$Q = q A_t = 10^{-6} \cdot 10^6 \text{ Pa.l/sec}$$

For a pressure at the pumps $p = 10^{-3}$ Pa, we get $S = Q/p = 10^3$ l/s which is the total pumping speed of the (turbomolecular) pump system. Eight 200 l/sec pumps, suitably distributed along the ring (with roughing pump added) are foreseen.

5.3. - Vacuum system summary.

- Vacuum chamber:

Material: S.S. AISI 304 L
 Size; bending magnets: rectangular 190x60 mm
 quadrupoles: circular \varnothing 150
 Area: 10^6 cm²
 Overall length: 70 m

- Vacuum system:

2000 l/sec distributed pumps inside bending magnets	8
400 l/sec titanium pumps	22
200 l/sec turbomolecular pumps	8
15 m /h roughing pumps with trap	8
Ionization vacuumeters (B.A. Type) ($10^{-1} \div 10^{-9}$ Pa)	22
Pirani type vacuumeters ($1000 \div 10^{-1}$ Pa)	8
Mass spectrometers	4
Gate valves	8

- Performance:

Pressure with turbomolecular pumps only	10^{-3} Pa
Pressure with titanium pumps	10^{-5} Pa
Pressure with titanium pumps after outgassing	2×10^{-6} Pa
Average pressure with beam without distributed pumping	6×10^{-7} Pa
Average pressure with beam with distributed pumping	$1 \div 2 \times 10^{-7}$ Pa
Pressure with beam in experimental straight sections.....	$1 \div 2 \times 10^{-6}$ Pa

5.4 - Particular care should be taken in avoiding sharp discontinuities in the vacuum chamber, to prevent too large higher order mode losses.

6. - Radiofrequency system

For a maximum energy $E_{\max} = 1.2$ GeV and a bending radius $\rho = 2.5$ m, the energy loss per

turn is:

$$eV = 88.5 \frac{E^4}{Q} = 73.4 \text{ KeV}$$

and for an overall beam current $I_f = 0,3 \text{ A}$ the power to be supplied to the beams (excluding higher order mode losses) is:

$$W_f = VI_f = 22 \text{ KW}$$

For a maximum cavity voltage $V_{\max} = 250 \text{ KV}$ and a $1 \text{ M}\Omega$ shunt impedance (R_S) the power loss to the cavity is:

$$W_C = V_{\max}^2 / 2 R_S = 31.25 \text{ KW}$$

The characteristics of the system are summarized in the following table.

-- Table 3 --

Frequency	51.4 MHz
Harmonic number	12
Number of cavities	1
Shunt impedance (R_S)	1 MΩ
Maximum voltage (V_{RF})	250 KV
Power to the beam (W_f)	22 KW
Power to the cavity (W_C)	31.25 KW
Beam current (I_f)	0.3 A

The power amplifier is identical to the existing 51.4 MHz ADONE system. A block diagram of the system is shown in fig. 8). A stabilizing loop on the cavity voltage and a feedback loop on "center-of-mass" oscillations are provided. A schematic cross section of the cavity, identical to that to be installed on ADONE, is shown in fig. 9): it is an aluminium cavity under vacuum.

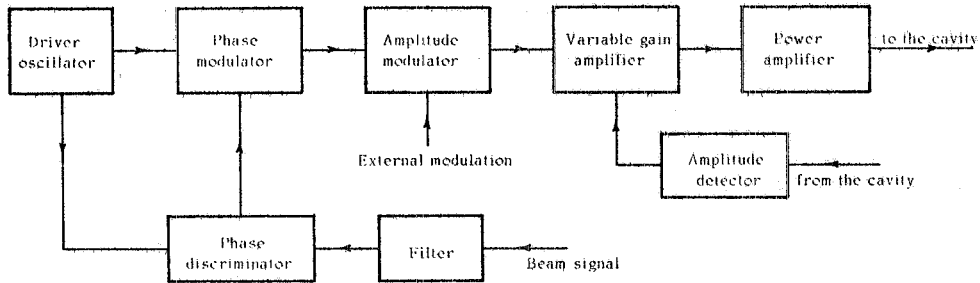


Fig.8 - RF system - Block diagram,-

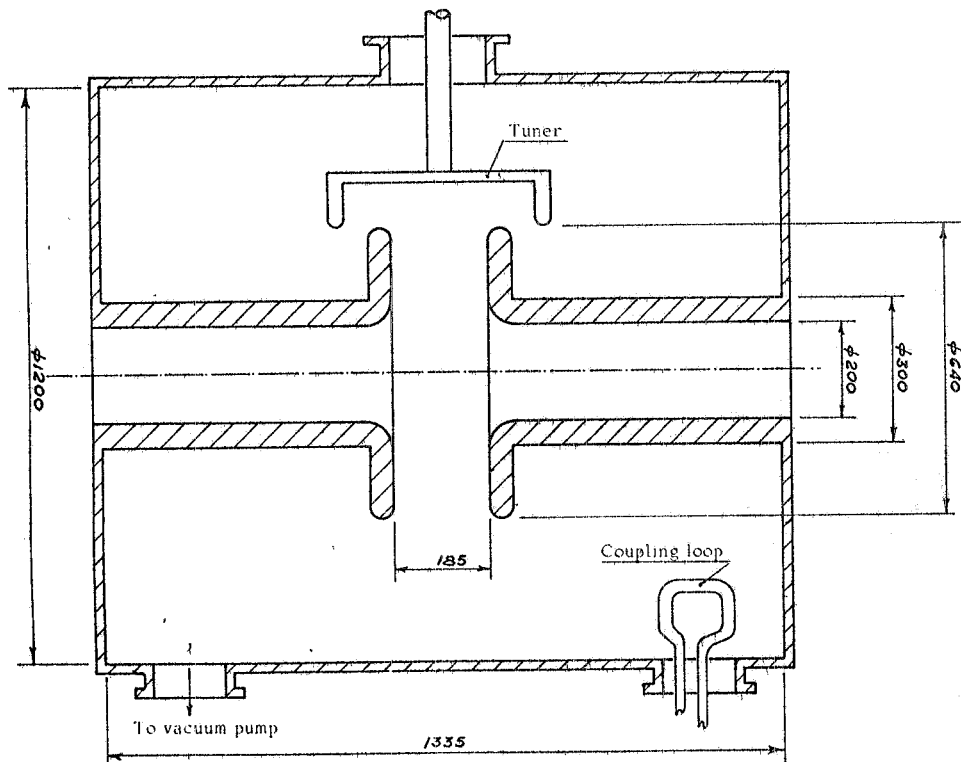


Fig.9 - R.F. cavity cross section.-

7. - INJECTION

7.1.- The injection hardware for ALA includes:

- 2 fast magnetic kickers³⁰⁾ which make a localized orbit bump in one of the two long straight sections, where the beams do not cross. The closed orbit in the rest of the ring is unperturbed, except for small errors.
- 2 magnetic septum deflectors³⁰⁾ (one for each beam), deflecting the incoming beam onto the perturbed orbit.

During injection and until the interaction configuration is reached, the beams must be separated at the interaction point. Separation is obtained by means of electric fields placed near the interaction straight sections.

The arrangement of kickers (SB), deflectors (D) and electrostatic plates (PS) for beam separation is shown in fig. 1. The main characteristics of the kickers and deflectors are listed in Table 4). The maximum electric fields required for beam separation are 10 KV/cm (for an interaction parameter $\xi = -.002$).³¹⁾

- Table 4 -

Element	E (MeV)	B1 (G.m)	L (m)	B (G.)	I (KA)	T/2 (μ s)	L (μ H)	C (μ F)	V (KV)
SB	450	220	1.4	150	5	~ 10	6	1.6	18
D	450	1800	1.45	1240	16	~ 80	.45	1000	.5

7.2.- Injection can be made directly from the LINAC, or using ADONE as a booster.

7.2.1. - Direct injection from the LINAC.

Given the current, emittance and energy spread of the beam delivered by our linear accelerator, electron injection is not a problem. The design current can be stored in a time of the order of a fraction of a minute.

The emittance of the positron beam at ~ 320 MeV is 10^{-5} m.rad and the energy spread $\pm .5\%$.³²⁾ Taking these figures into account, the aperture needed for injection in the region outside the "injection bump" is compatible with that indicated in 3.4.1, but, particularly in the horizontal direction, without any safety margin. Moreover, the aperture of the 4 quadrupoles inside the injection bump (and the 4 opposite ones) must be increased to 200 mm.

Scaling from the maximum injection rate achieved on ADONE with its 8.57 MHz RF cavity, the expected injection rate is of the order of 20 mA/min, assuming there is an auxiliary 8,57 MHz RF cavity on ALA too. Since, with the indicated aperture, the injection efficiency is expected to drop by a factor of 2 to 3, positron injection time at 320 MeV may become as long as ~ 25 minutes.

7.2.2. - Injection from ADONE.

The sequence of operations is the following:

- a) Injection of three bunches in ADONE.
- b) Extraction of single bunches from ADONE.
- c) Transfer and injection in a single bunch of ALA.

Extraction from ADONE has already been extensively discussed;⁵⁾ it requires the installation of

a fast kicker and a septum magnet in two consecutive straight sections (e.g. number 10 and 11). Electron injection is performed directly from the LINAC.

The characteristics of the ADONE beam (emittance $\sim 2 \times 10^{-8}$ m.rad, energy spread $\sim 2 \times 10^{-4}$) ask for an aperture much smaller than that indicated in 3.4.1 (needed for the interaction configuration), which is therefore more than adequate.

With the ADONE injection rate (8.57 MHz RF cavity) and assuming to transfer to ALA at the ADONE injection energy (without acceleration) the achievable injection rate in ALA is of the order of 30 mA/min, assuming 100% injection efficiency. The last assumption is very reasonable when a damped bunch is injected in a single turn.

- 7.2.4. - It is clear that, from the machine point of view, injection from ADONE is preferable. In the final design stage, the two solutions will however have to be compared taking into account costs and interference with other ADONE activities. In particular for direct injection from the LINAC a more detailed study of injection efficiency is required, considering also the possibility of installing an "energy compressor" to bring the energy spread to values of the order of $\pm .1\%$, and/or of increasing the LINAC maximum energy.

8. - CONTROL SYSTEM

- 8.1. - The control system includes:

- a) Equipment supervision (power supplies, vacuum, RF, etc.)
- b) Beam diagnostic and control
- c) General services (alarms, protections, communications, etc.).

The architecture of computer-controlled systems is by now relatively standard,^{5), 33)} and a detailed discussion is unnecessary at the present design stage.

The characteristics of the ALA beam are similar to those of ADONE so that the need for development of completely new techniques should not arise.

- 8.2. - Since the size of the ring is relatively small, the control system can be built around a single computer.³⁴⁾

The principal characteristics of the system should be:

- a) Maximum hardware flexibility, by the use of modular standard dataways (IEEE 488-1975 or CAMAC).
- b) Maximum software flexibility, obtained by one or more mass-memory units coupled with an interpreter language.
- c) Easy communication with operators.

Fig. 10) shows an example of configuration which fulfills the above requirements.

The relatively low cost of read-write and mass memories justifies their overdesign, allowing for a higher flexibility in the development of control software and a higher program execution speed.

The operating system should allow for real time multiprogramming, in order to avoid programming and debugging dead times.

- 8.3. - A good beam control and diagnostic system is essential to obtain the best storage ring performance.

The system should include:

- On-line measurement and correction of closed orbit (24 measuring sections, precision $\lesssim 1$ mm, ≥ 12 correction coils).
- Measurement of beam size by synchrotron radiation.
- Transverse feedback.
- Longitudinal feedback on the "center-of-mass" mode.
- Luminosity measurement by Bhabha scattering.
- Accurate position and intensity measurement along the transport channels (20 stations).

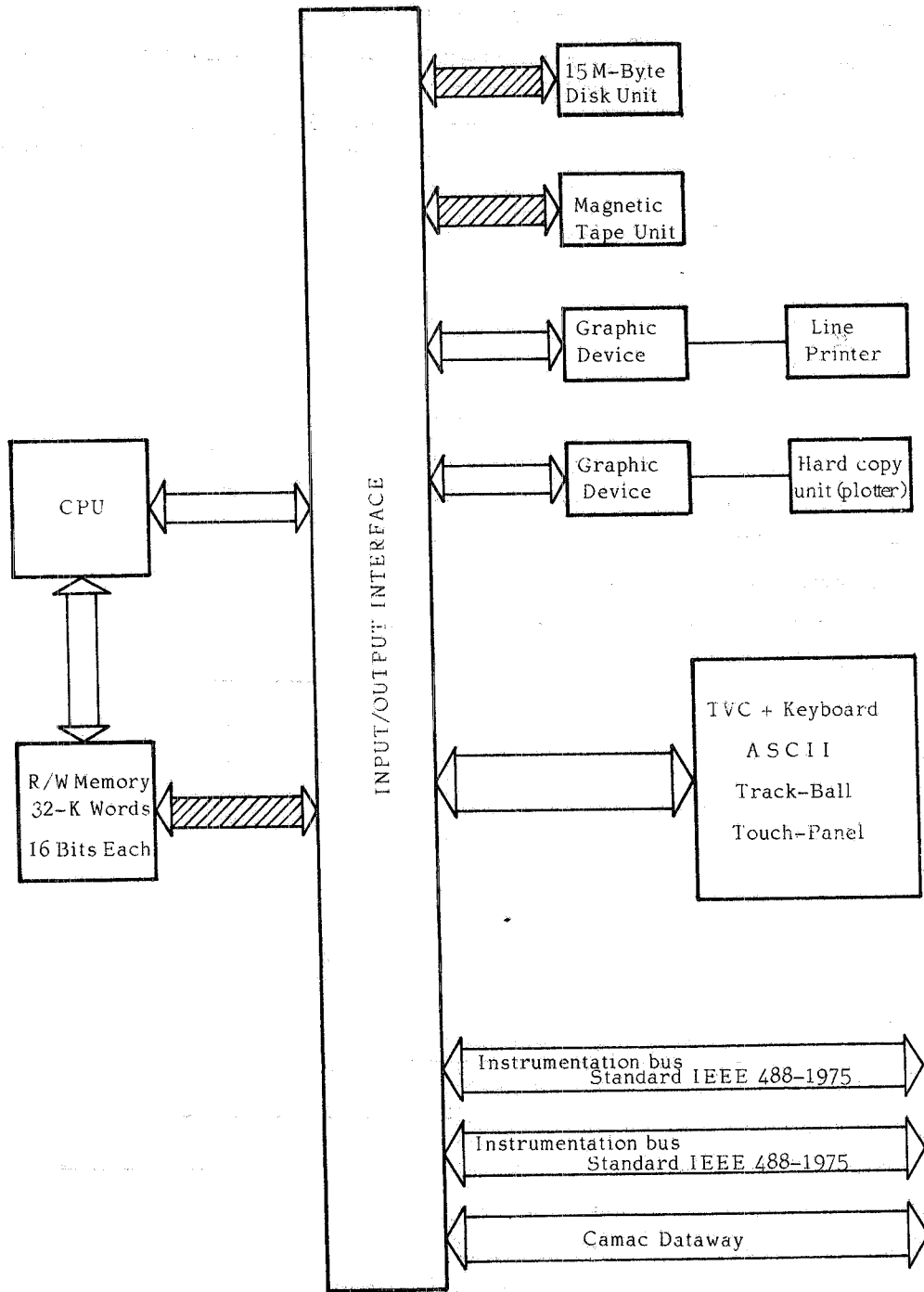


Fig.10 - Main control unit - Block diagram.-

9. - BUILDINGS AND UTILITIES

Given its size, the ring can be easily located within the Frascati National Laboratories area dedicated to future developments.

Water and electric power requirements can also be easily met.

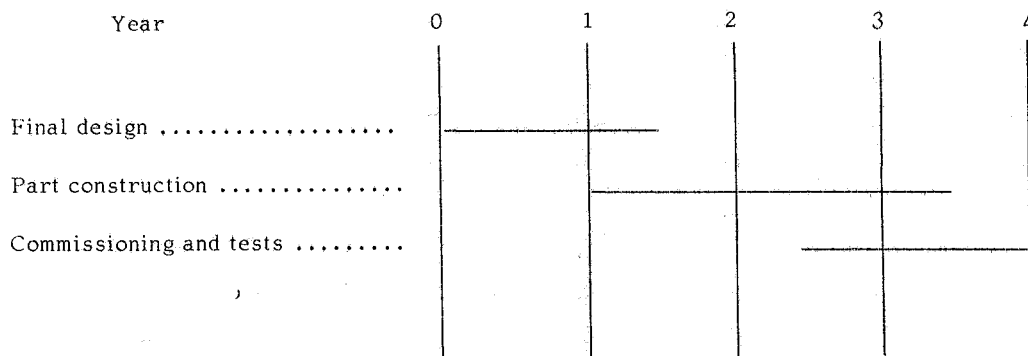
At the present stage of the project the exact location of the ring and service buildings has not been defined. In estimating costs, economy was a main concern.

The buildings include a 12x8x11 m³ experimental hall, equipped with a 25 tons crane. For the ring, a ring shaped prefabricated structure, with side access, without crane and with outside shielding is proposed.

10. - COST ESTIMATE (in MLit - 1977)

- Magnet	1.200
- Power supplies	300
- R.F.	200
- Vacuum	400
- Injection	300
- Beam transfer	400
- Controls	700
- Buildings	700
- Utilities	400
	<hr/>
	4.600
	=====

11. - TIME SCHEDULE



A.L.A.--Parameter summary

BEAM CHARACTERISTICS					
Energy (GeV)5	.62	.78	1	1.2
Luminosity x 10 ³¹ (cm ⁻² s ⁻¹)	1 bunch per beam				
	.15	.36	.90	1.17	1.4
Total current (mA)	2 bunches per beam				
	.30	.72	.90	-	-
Total current (mA)	1 bunch per beam				
	40	75	150	150	150
Energy loss per turn (KeV)	2 bunches per beam				
	80	150	150	-	-
Energy loss per turn (KeV)	2.2	5.2	13.1	35.4	73.4
R.m.s. dimensions at crossing (mm)	horizontal out of coupling (1b/beam)				
	.67	.83	1.04	.92	.84
	vertical on coupling (1b/beam)				
Lifetime (beam/beam bremsstrahlung + gas bremsstrahlung) (hours).....	.18	.23	.29	.27	.26
	longitudinal (radiation only, V _{RF} = 250 KV 1b/beam)				
Center of mass energy resolution (FWHM, MeV)	49	67	95	103	117
Lifetime (beam/beam bremsstrahlung + gas bremsstrahlung) (hours).....	16	14	12	11	10
Center of mass energy resolution (FWHM, MeV)45	.69	1.10	1.80	2.59

MAGNETIC STRUCTURE		
Orbit length (m)	70	
Average radius (m)	11.14	
Experimental straight section length (m)	3	
Periodicity	2	
Bending radius (m)	2.5	
Maximum bending field (Tesla)	1.6	
Quadrupole length (m)5	
Maximum gradient (Tesla/m)	8	
Total weight (tons)	Fe 96	Cu 6.0
	Fe 15.1	Cu 6.7
Magnet aperture (cm ²)	7 x 15	
Quadrupole free diameter (cm)	7.5	

FOCUSING CHARACTERISTICS		
	Interaction configuration	Injection configuration
Horizontal betatron frequency (Q_x)	3.2	3.2
Vertical betatron frequency (Q_z)	3.2	3.2
Invariant (M) m80 ± 2.28	.55
Invariant at crossing (M^*) m81 ± 3.00	.80
Momentum compaction (α_c)10 ± .25	.036
Horizontal betatron wavelength at crossing (β_x^*) m	1	3
Vertical betatron wavelength at crossing (β_z^*) m2	1
Dispersion at crossing (ψ^*) m	-.16 ± -1.21	1.2
β_x^{\max}	26.9 ± 27.4	17.9
β_z^{\max}	13.3 ± 15.3	24.5
ψ^{\max}	4.0 ± 5.1	4.3
Horizontal chromaticity ($p\Delta v_x/v_x\Delta p$)	-2.30 ± -2.67	-1.38
Vertical chromaticity ($p\Delta v_z/v_z\Delta p$)	-1.53 ± -1.91	-1.77

RADIOFREQUENCY SYSTEM	
Frequency MHz	51.4
Harmonic number (h)	12
Number of cavities	1
Maximum power to the beam KW	22
Power to the cavity KW	250
Maximum cavity voltage KVolt	1
Shunt impedance $M\Omega$	1

VACUUM SYSTEM	
400 l/s titanium pumps	22
200 l/s turbomolecular pumps	8
Distributed pumps inside bending magnets (15 m total length)	8
Average pressure with beams (Torr)	$.75 \times 10^{-9} \div 1.5 \times 10^{-9}$
Average pressure with beams in experimental straight section (Torr)	$.75 \times 10^{-10} \div 1.5 \times 10^{-10}$

INJECTION		
	Direct from LINAC	Through ADONE
Injection energy (MeV)	300 ± 450	300 ± 450
Horizontal emittance at injection point (mm x mrad)	10	$1.5 \times 10^{-2} \div 3.5 \times 10^{-2}$
Vertical emittance at injection point (mm x mrad)	10	$3.5 \times 10^{-4} \div 8.2 \times 10^{-4}$
Positron injection rate (mA/min)	~5	~30
Electron injection rate (mA/min)	150	-

APPENDIX 1.

A.1. - Machine performance could be further improved by raising the RF frequency. A higher frequency would shorten the bunch length (which is itself an advantage for physics experiments) allowing to make β_z^* shorter and therefore increase the luminosity.

A preliminary discussion on the choice of the RF frequency and on the range of parameters to be expected is given.

A.2. - General remarks.

A high RF frequency associated with an optical structure having non zero dispersion at the places where cavities are located raises the problem of the excitation of synchro-betatron resonances since the synchrotron oscillation wavenumber tends to become comparable with the fractional part of the radial betatron wavenumber. Also, if the bunch becomes so short that losses due to higher order modes in the cavities and in the vacuum chamber become comparable to the natural radiation loss, besides having to supply more power to the beams, one also has to increase the RF voltage, thereby again increasing the synchrotron wavenumber. Last, direct injection from the LINAC becomes more difficult due both to the reduced time acceptance of the machine and to other effects, such as Touschek lifetime, coming into play at low energy.

Detailed calculations of all these effects will have to be carried out before arriving at a final decision on the RF frequency. At this stage of the design it seems that a frequency of around 100 MHz is reasonable. Five hundred MHz, that would be desirable because of the large amount of experience made on it at DESY, seems at present too high.³⁶⁾

In the performance study that follows we assume that the RF frequency is 102.8 MHz.

A.3. - Optics and aperture.

The optics described in Section 3 easily allows for β_z^* to be made as low as 10 cm, with only minor modifications.³⁷⁾ The resulting optical functions in the two extreme operating configurations are shown in figs. A1, A2.

Obviously β_z in first quadrupole near the crossing region is much higher, but in the rest of the machine β_x and β_z are practically unchanged.

The apertures required for operation are still compatible with those specified in the text, and are shown in figs. A3, A4.

The natural radial and vertical chromaticities, shown in fig. A5, are higher than those for $\beta_z^* = 20$ cm but can be corrected with the same sextupole arrangement.

A.4. - Radiofrequency system.

The main parameters of a possible RF system are listed in Table A1.

- TABLE A1 -

Frequency	102.8 MHz
Harmonic number	24
N. of cavities	1
Cavity length	1 m
Maximum RF voltage	400 KVolt
Shunt impedance	4.5 M Ω
Maximum power to the cavity	14 KW
Maximum power to the beam	26 KW

A first estimate of the higher mode losses, scaling from SPEAR II numbers³⁶⁾, and assuming the effective chamber impedance per unit length is made ten times lower by a careful chamber design, indicates that the overall loss (cavity + vacuum chamber) should be of the order of 3KW for a 6 cm bunch length. The RF voltage shown in Fig. A6 includes this loss.

A.5. - Bunch length.

Since the synchrotron wavenumber increases with RF voltage, it seems necessary, in order to avoid synchro-betatron resonances (see A.2) to vary the RF voltage as a function of energy. The RF voltage needed to obtain a fixed natural bunch length of 6 cm at all energies is shown in fig. A6, RF energy acceptance and total power are also shown as a function of energy in Fig. A6.

An estimate of the anomalous bunch lengthening, according to the Chao-Gareyte model¹⁷⁾ and using parameters scaled from the SPEAR results, indicates that bunch lengthening should be negligible at the operating currents; it has of course to be kept in mind that such estimates may be accurate up to a factor of the order of 1.5.

Comparing the source length with that obtained, by the same procedure, for a 51.4 MHz cavity, it can be seen that the gain factor on source length varies between ~ 1 and 2 depending on energy.

More detailed studies of synchro-betatron resonances (and their possible cures) and higher order mode losses are needed to decide whether it is possible to do better.

A.6. - Luminosity and lifetime.

According to formula (1) of the text (§ 2.2) by lowering β_z^* by a factor of two an increase of luminosity by approximately the same factor should be obtained ($\beta_x^* \gg \beta_z^*$). Actually to stay away from synchro-betatron resonances it could be necessary to increase the fractional part of the betatron tune, so that ξ_m could drop from .06 to $\sim .05$. If this will be the case, luminosity will increase, over that computed for 51.4 MHz, by a factor of ~ 1.4 only. Expected luminosity is plotted versus energy in fig. A7.

Fig. A8 shows the gas bremsstrahlung and beam-beam bremsstrahlung lifetimes.

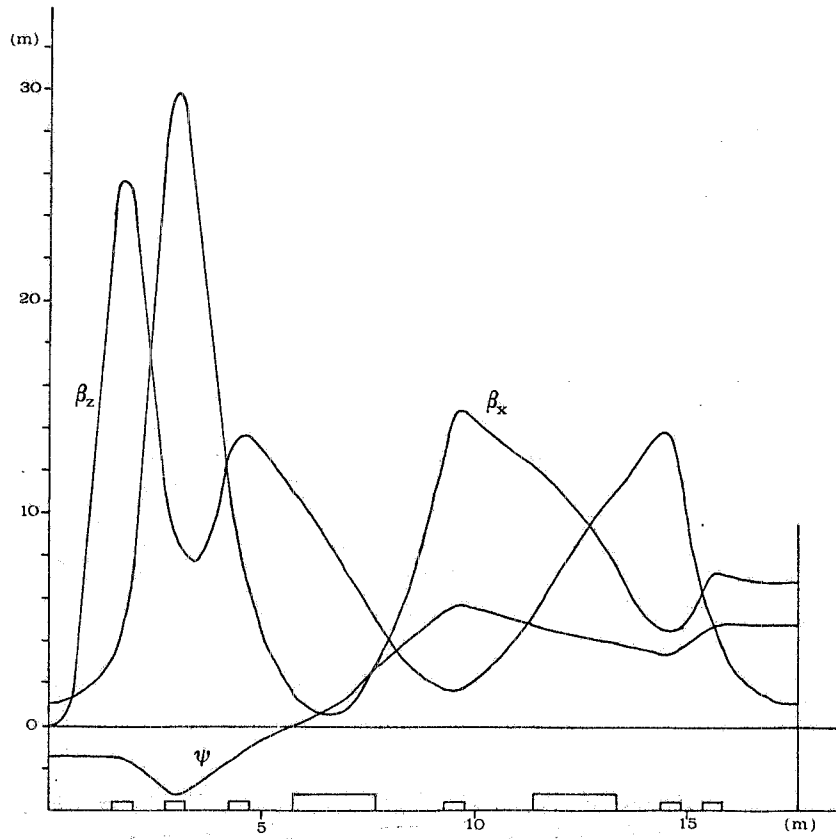


Fig. A1 - Optical functions for $\beta_z^* = 10$ cm - $M^* = 3.62$ - $\alpha_c = .25$ - $E \leq 730$ MeV

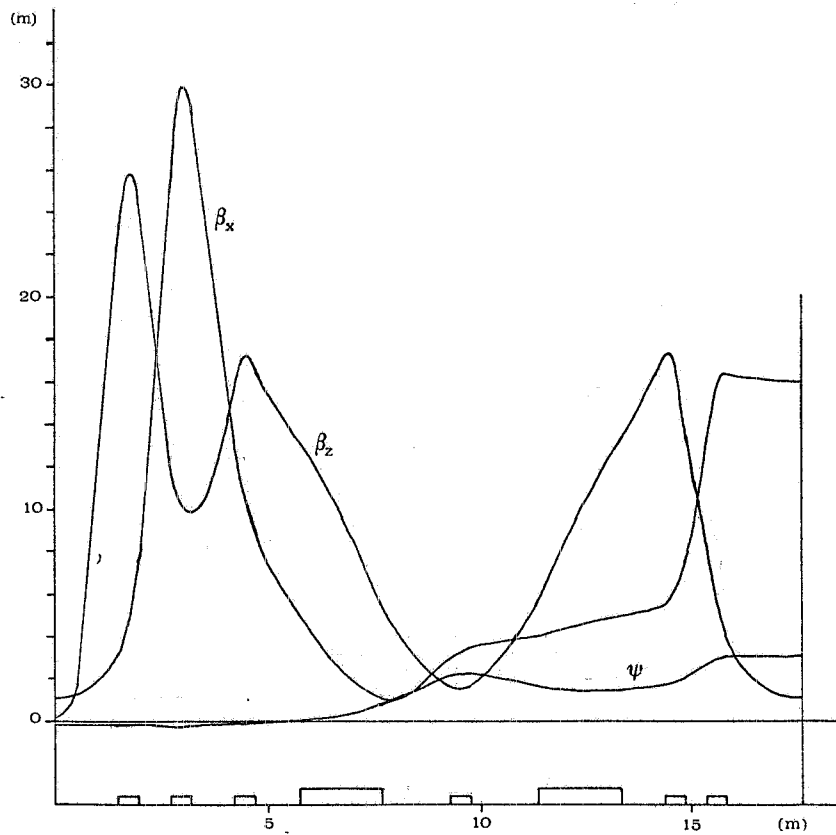


Fig. A2 - Optical functions for $\beta_z^* = 10$ cm - $M^* = .82$ - $\alpha_c = .08$ - $E = 1200$ MeV

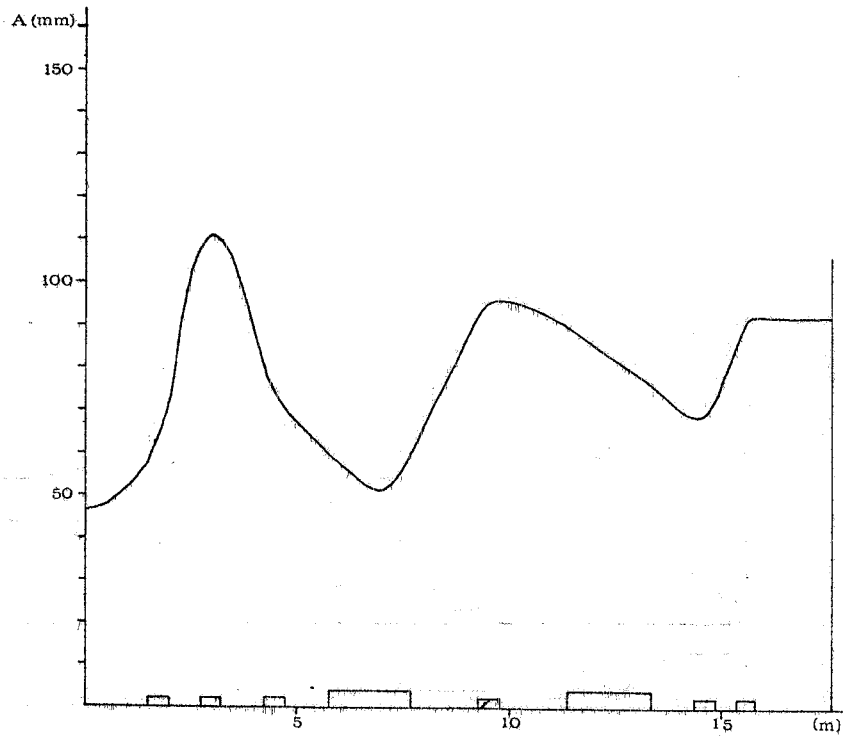


Fig. A3 - Horizontal aperture

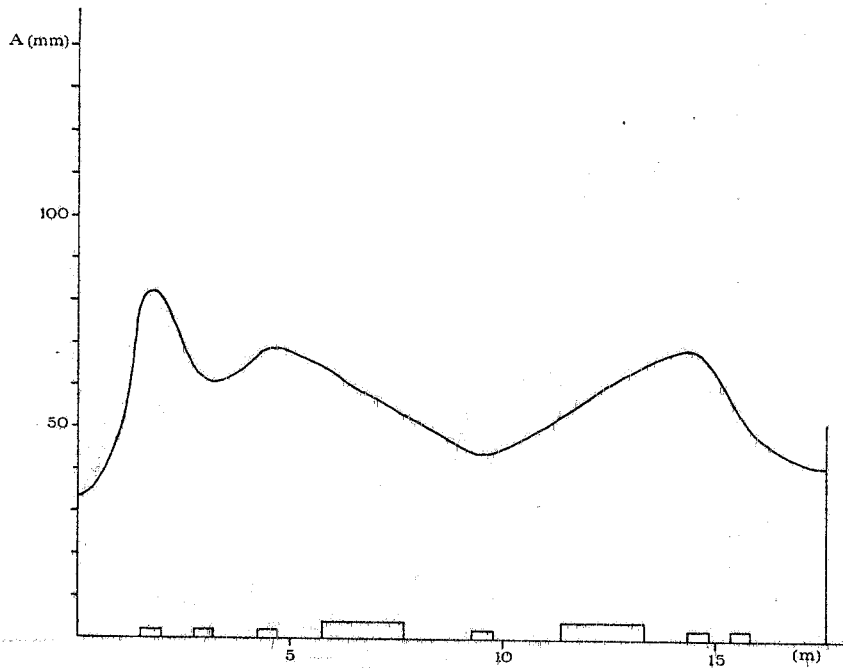


Fig. A4 - Vertical aperture

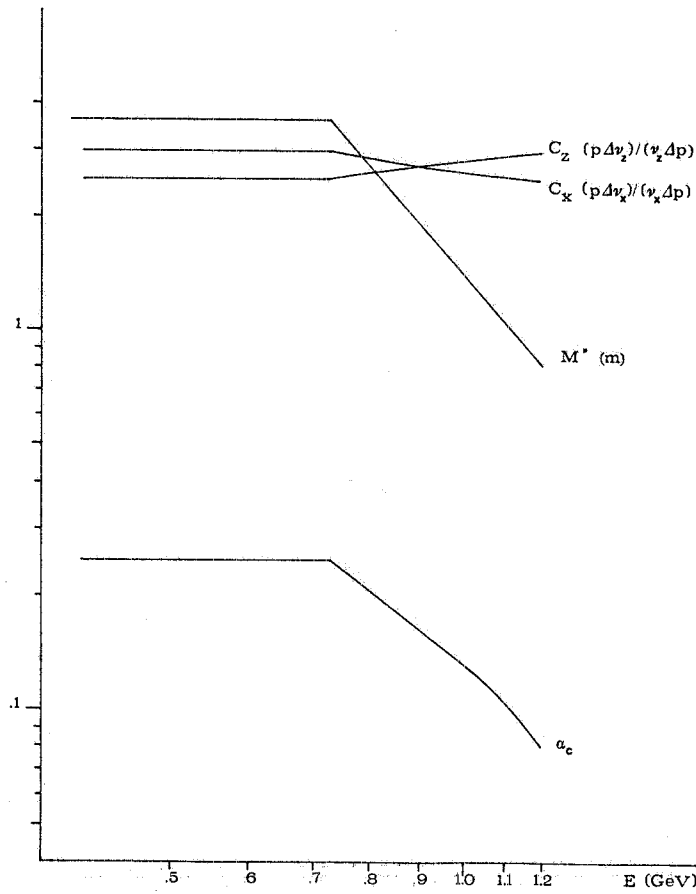


Fig. A5 - Invariant M^* , horizontal and vertical chromaticity, momentum compaction

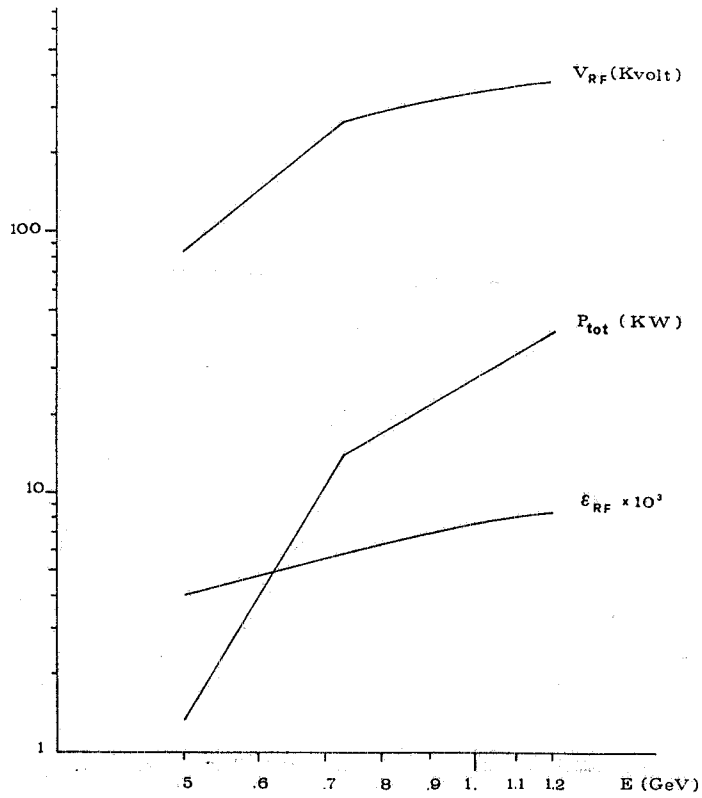


Fig. A6 - RF voltage, total power and energy acceptance

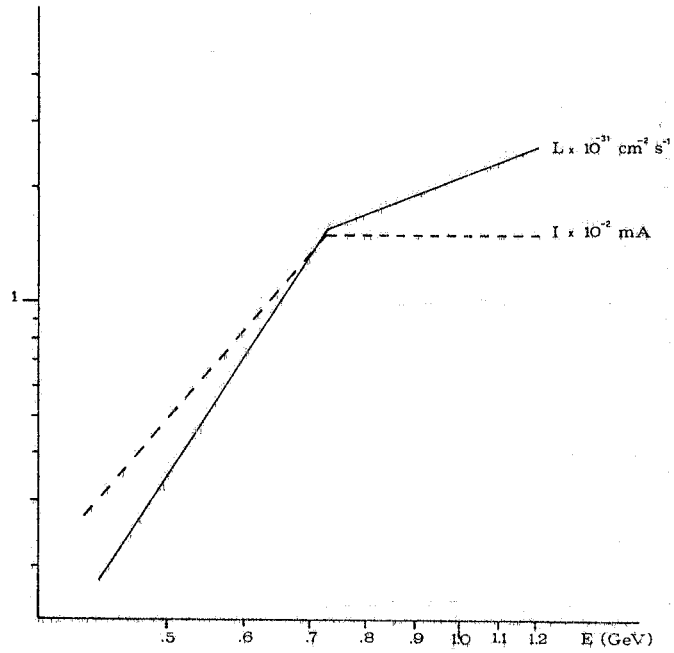


Fig. A7 - Luminosity per crossing and current per beam

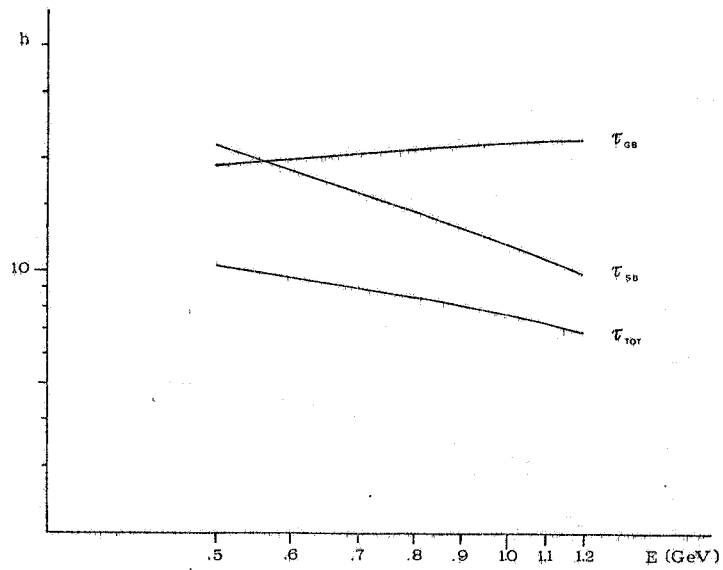


Fig. A8 - Single beam-beam (τ_{sb}), gas (τ_{gb}) and total (τ_{tot}) bremsstrahlung lifetime

REFERENCES

- 1) - Proposta per un anello di accumulazione per elettroni e positroni a luminosità alta (ALA) e per la misura accurata delle proprietà delle risonanze di massa $1100 \lesssim M_{e^+e^-} \lesssim 2200$ MeV prodotte nella annichilazione elettrone-positrone. LNF 77/3 (Int.) (1977).
- 2) - M. Bassetti "Un modo di cambiare l'invariante M" Adone Int. Memo T-56 (1973).
M. Bassetti "Variable $1/Q$ curvature function storage rings. Dimensions and damping control" Adone Int. Memo T-66 (1974).
- 3) - Petra - Updated version of the Petra proposal - DESY (1976).
- 4) - "A proposal for a positron-electron colliding-beam storage ring project (PEP)" - SLAC 171, LBL 2688 (1974).
- 5) - "Super Adone design study" INFN-LNF (1974).
- 6) - A.N. Skrinsky "Electron-positron storage rings at the Institute of Nuclear Physics, Novosibirsk" Invited talk (review) given at the USSR Accelerator Conference, Dubna (1976).
- 7) - F. Amman "Electron-positron storage rings: present situation and future prospects" Proceedings of the 8th International Conference on High Energy Accelerators - CERN pag. 63 (1971).
- 8) - Spear Storage Ring Group "Spear: Status and improvement program" IX International Conference on High Energy Accelerators, Stanford - pag. 37 (1974).
- 9) - DESY Storage ring group "DORIS: Present status and future plans" IX International Conference on High Energy Accelerators - Stanford - pag.43 (1974).
- 10) - The Orsay Storage Ring Group "Status Report on D.C.I." RT-2/77 - X International Conference on High Energy Accelerators - Serpukhov (1977).
- 11) - F. Amman "Longitudinal instability due to beam-beam interaction in electron storage rings" LNF 71/782 (1971).
- 12) - M.E. Biagini "Cammino dal punto di iniezione al punto di lavoro per ALA" Adone Int. Memo T-90 (1978).
- 13) - R. Belbeoch et al. "Proceedings of the National Conference on Particle Accelerators" Moscow - p.129 (1968).
- 14) - F. Amman et al. "Proceedings of the VIII International Conference on Particle Accelerators" p.68 Geneva (1971).
- 15) - M.A. Allen et al. "Proceeding of the IX International Conference on Particle Accelerators" p. 352 Stanford (1974).
- 16) - A.W. Chao, Y. Gareyte "Scaling law for bunch lengthening in SPEAR II" SPEAR-197/PEP-224 (1976).
- 17) - S. Tazzari "Scaling dell'allungamento anomalo secondo il modello Chao e Gareyte" Adone Int. Memo T-93 (1978).
S. Guiducci, G. Martinelli "Lunghezza dei bunches e allungamento anomalo per ALA" Adone Int. Memo T-89 (1978).

- 18) - M. Preger, S. Tazzari "ALA 5 - Struttura a M variabile - Calcolo delle aperture necessarie" Adone Int. Memo SM-18 (1978).
- 19) - W. Hardt, R.D. Kohaupt "On bunch lengthening and the Particle Distribution in Electron Storage Rings" DESY Internal Report PET-77/03 (1977).
- 20) - S. Tazzari "Apertura per l'iniezione - ALA" Adone Int. Memo EI-4 (1978).
- 21) - C. Pellegrini "On a new instability in electron-positron Storage Rings (the head-tail effect)" Il Nuovo Cimento 64 A p.447 (1969).
- 22) - M. Preger "Campi sestupolari necessari per la correzione del cromatismo in ALA" Adone Int. Memo SM-19 (1978).
- 23) - M.H.R. Donald, P.L. Morton, H. Wiedemann "Chromaticity correction in large storage rings".
- 24) - M. Bassetti "Perturbative method for chromatic and sextupolar effects. 2nd order solution" Technische Notiz PET-77/35, DESY Hamburg (1977).
- 25) - C. Sanelli "ALA: Alimentazioni" Adone Int. Memo MA-36 (1978).
- 26) - A. Cattoni, G. Corazza, A. Marra "Risultati delle misure effettuate per l'allineamento del magnete" LNF 67/47 (Int.) (1966).
- 27) - A. Cattoni "Considerazioni preliminari sull'allineamento del Super Adone" Adone Int. Memo MM-7 (1973).
- 28) - A. Cattoni "ALA - Struttura magnetica: Magnete curvante" Adone Int. Memo MA-35 (1978).
- 29) - A. Cattoni "ALA - Struttura magnetica: Lenti quadrupolari" Adone Int. Memo MA-34 (1978).
- 30) - R. Boni, F. Tazzioli "Sistema di iniezione per ALA" Adone Int. Memo D-8 (1978).
- 31) - M. Preger "Campi elettrici necessari per la separazione dei fasci in ALA" Adone Int. Memo SM-20 (1978).
- 32) - F. Amman, R. Andreani "L'acceleratore lineare per elettroni e positroni" LNF 63/46 (1963).
- 33) - M.C. Crowley-Milling "The control system for SPS" CERN Lab. II - CO/74-1 (1974).
- 34) - E. Fiorentino, M. Serio, F. Tazzioli "ALA: Sistema di controllo - discussione preliminare" Adone Int. Memo SC-90 (1978).
- 35) - A. Piwinski, A. Wrulich "Excitation of Betatron-Synchrotron resonances by a dispersion in the cavities" DESY 76/07 (1976).
- 36) - M. Preger, S. Tazzari "Criteri per la scelta della frequenza RF per ALA" Adone Int. Memo RF-36 (1978).
- 37) - M.E. Biagini, M.A. Preger "ALA 6 - Struttura con $\beta_z^* = 10$ cm" Adone Int. Memo SM-22 (1978).
- 38) - P.B. Wilson "Stored current in PEP at 125, 200 and 358 MHz" PEP-123 (1975).